nzsee
NEW ZEALAND SOCIETY FOR EARTHQUAKE ENGINEERING

Estimates of site periods from mHVSR analysis of IRIS temporary seismograph networks

A.C. Stolte, C. Brown, K.L. Lee & L.M. Wotherspoon
University of Auckland | Waipapa Taumata Rau, Auckland, New Zealand.

E.F. Manea
GNS Science | Te Pū Ao, Lower Hutt, New Zealand.

National Institute for Earth Physics, Măgurele, Ilfov, Romania.

ABSTRACT

The effects of soil stratigraphy and sedimentary basins on earthquake ground shaking are well-established. These effects can be represented using a range of site metrics, with the focus of this paper being the fundamental period of vibration of soil above bedrock (T_0). T_0 has been used to differentiate between sub-soil site class C and D in NZS1170.5 and in the seismic microzonation of sedimentary basins as a proxy for basin depth. An increasingly common method to estimate site period is via identification of peaks in the Horizonal-to-Vertical Spectral Ratio of microtremor (mHVSR) data. Several recent studies in Aotearoa New Zealand and internationally have focused on the temporary deployment of sensors to characterise sedimentary basins on local and regional scales. This paper leverages a dataset of ambient vibration recordings from several studies collected using instrumentation borrowed from the Incorporated Research Institutions for Seismology (IRIS). Broadband seismometers have been deployed at 785 locations across the country. Data was publicly available at 311 sites and suitable for mHVSR analysis at 113 sites. New estimates for site period are presented herein for sites across the country, including Southland, Otago, along the Alpine Fault, and throughout the Taupō Volcanic Zone. All provide insight into sedimentary basin and earthquake ground shaking.

1 INTRODUCTION

The effects of soil stratigraphy and strong impedance contrasts between soft soil layers and stiff rock are well known in the practice of geotechnical earthquake engineering. Observations of ground shaking in sedimentary basins have shown amplified and prolonged ground motions due to entrapment of the seismic waves and the generation of localised surface waves (Borcherdt 1970, Kramer 1996). An ongoing area of research is the characterisation of sedimentary basins, understanding their effects on ground shaking, and incorporating these findings into ground motion models.

Site effects are often modelled using simplified metrics. Common metrics include the time averaged shear wave velocity over the top 30 metres (V_{S30}) and depth to layers with shear wave velocities of 1.0 km/s and 2.5 km/s ($Z_{1.0}$ and $Z_{2.5}$, respectively). V_{S30}, $Z_{1.0}$, and $Z_{2.5}$ are included in recent ground motion models (GMMs), such as the NGA-West2 (Gregor et al. 2014). However, in Aotearoa New Zealand there is a paucity of available $Z_{1.0}$ and $Z_{2.5}$ data and measurement of these values is challenging as competent rock is often very deep (Wotherspoon et al. 2022). Another common metric is the fundamental site period (T_0). It is directly related to the bedrock depth, whose interface to soft sediments is responsible for the development of destructive resonance phenomena (Manea et al., 2020). The ability of T_0 to capture site effects is well-known (Cadet et al, 2012) and it is often used together with V_{S30} (Pitilakis et al, 2013; Zhu et al., 2020; Manea et al., 2022). A T_0 of 0.6 s is used to delineate the boundary between site classes C (shallow soil) and D (deep/soft soil) in the Aotearoa New Zealand seismic design standards, NZS1170-5:2004 (SNZ 2004).

The horizontal-to-vertical spectral ratio of ambient vibration records (sometimes called microtremors) (mHVSR) at a single station has seen increased usage for estimation of T_0. The method is simple both in data acquisition and analysis. It has been used for characterisation of sedimentary basins in Aotearoa New Zealand and internationally. Nogoshi and Igarashi (1971) initially studied microtremors and explored the cause of peaks mHVSR spectra. Nakamura (1989, 2019) proposed the use of mHVSR to characterize site effects and popularized the method. With the increasing use of mHVSR testing for site characterisation, the SESAME European Research Project developed guidelines for the implementation of the method (SESAME 2004) and Molnar et al. (2018) provided recommendations for data acquisition and analysis.

This paper presents T_0 estimates from mHVSR analysis using existing, publicly available ambient vibration measurements from the temporary deployment of broadband seismometers across Aotearoa New Zealand. A summary of nationwide results is presented and mHVSR spectra from measurements in the Taupō Volcanic Zone detailed. The implication of multiple peaks in mHVSR spectra are briefly discussed.

2 AMBIENT VIBRATION DATA AND ANALYSIS

2.1 Data from IRIS Repository

The Incorporated Research Institutions for Seismology (IRIS) comprises of 100+ US-based and 50+ international research institutions is funded by the United States National Science Foundation. Through the IRIS Program for Array Seismic Studies of the Continental Crust (PASSCAL) and EarthScope USA Array Operations Facility (AOF), researchers worldwide may borrow broadband sensors for deployment of temporary arrays. Any data collected using IRIS instrumentation must be made publicly available on the IRIS data service (https://service.iris.edu/), after research publication embargoes.

Over the past 30 years, IRIS instrumentation has been used for several studies in Aotearoa New Zealand at 785 sites both on- and off-shore. Deployments ranged in duration from days to years. These data were downloaded from the IRIS data service using an FDSN client. An attempt was made to download a single day of ambient vibration data for each site. Data were non-embargoed, available, and successfully downloaded for 311 sites. Each of the records was assessed for suitability for mHVSR analysis in the present study. Only sensor deployments onshore were considered suitable. Additionally, records with errors or missing components (vertical and two orthogonal horizontal components required) were removed. Of the 311 downloaded records, a subset of 113 records were deemed usable.

2.2 HVSR Analysis

The day-long ambient vibration records were processed using the hvsrpy python package (Vantassel 2020). The North-South (NS) horizontal, East-West (EW), and Vertical (VT) components of an example day-long ambient vibration record are shown in Figures 1a, 1b, and 1c, respectively. The records were not filtered and

each record was broken into 720 two-minute-long windows. A cosine taper of 10% of the window length was applied to each detrended window. The windowed timeseries for each component was transformed into the frequency domain. The two horizontal components were combined by evaluating the geometric mean on a frequency-by frequency basis. The frequency domain points were resampled to 200 frequency values evenly spaced on a log-scale between 0.1 and 20 Hz. Konno and Ohmachi (1998) smoothing with a bandwidth constant of 40 was applied in the frequency domain. The ratio between Fourier amplitude spectra of the combined horizontal components and the vertical component was then evaluated.

For each time window, hvsrpy identifies the maximum amplitude in the mHVSR spectra. The frequencies associated with strong mHVSR peaks have been shown to be associated with the fundamental frequency (f_0), or period (T_0), of vibration of the soil/rock strata above a stiff layer. f_0 (and T_0) are assumed to be lognormally distributed. Initially, the lognormal mean and standard deviation (σ_{ln}) of f_0 for all windows is evaluated, as shown in Figure 1d. The frequency-domain window-rejection algorithm (Cox et al. 2020) is used reject outlier time windows with peak frequency values outside the ±2 σ_{ln} bounds. For the example

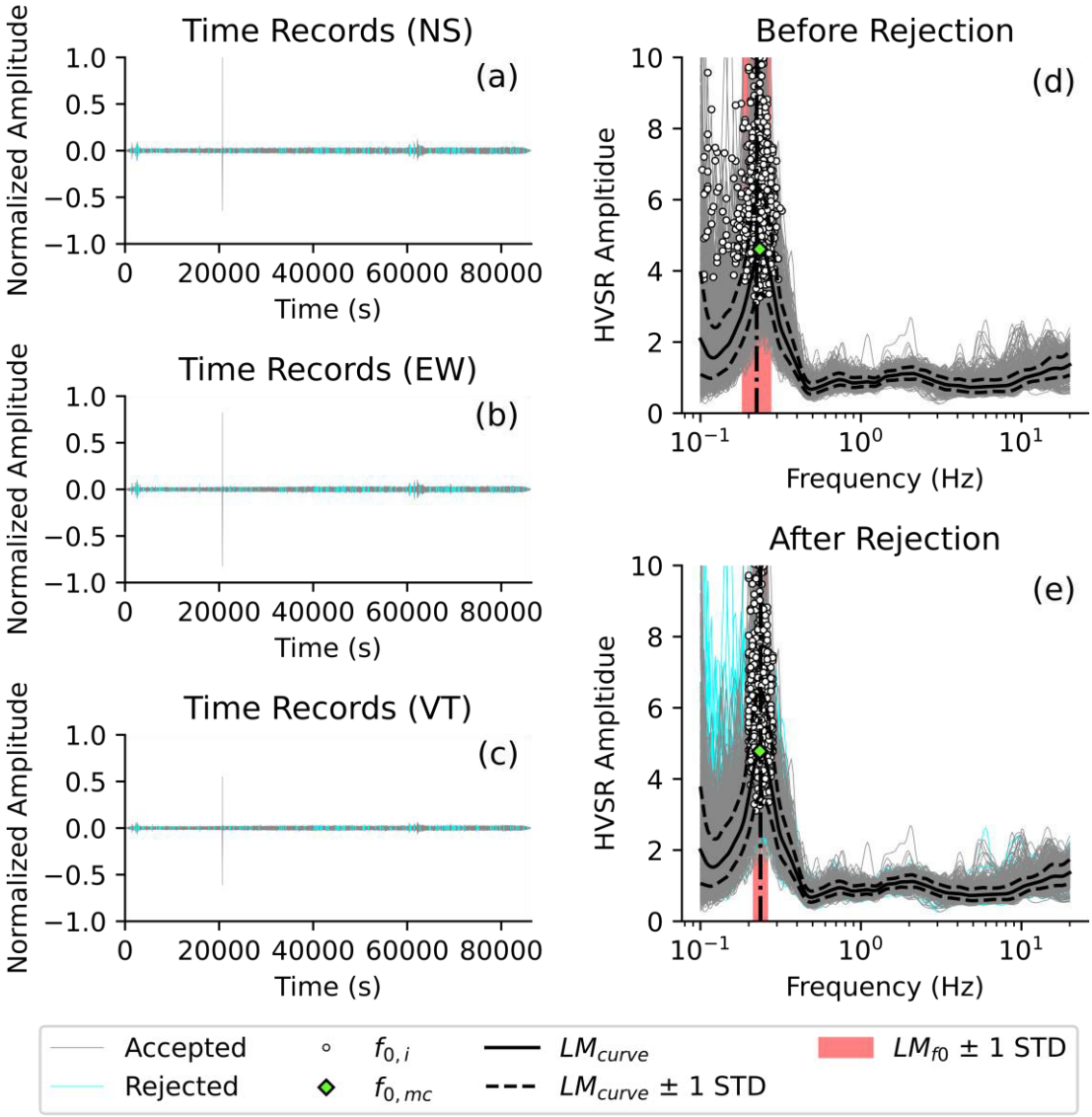

Figure 1: Example mHVSR analysis of a day-long ambient vibration data extracted from the IRIS data repository. (a) North-South horizontal, (b) East-West horizontal, and (c) vertical time records are windowed and processed to develop mHVSR spectra, (d) before and (e) after rejection of outlier time windows.

record in Figure 1, 123 of the 720 windows were rejected (as indicated by cyan lines) and excluded from the final f_0 statistics. In this case, the lognormal mean f_0 is 0.24 Hz, the associated T_0 is 4.22 s, and the σ_{ln} for both is 0.09. Each mHVSR peak was assessed using the SESAME (2004) criteria. Only peaks passing three of three SESAME reliability criteria, passing at least four of six SESAME clarity criteria, and having a mHVSR amplitude greater than 2 were kept for subsequent analysis.

For each of the 113 temporary ISIS deployments with suitable data, the mHVSR spectra were calculated and peaks were identified. At some sites, no clear peak in the mHVSR spectra could be identified, such as the example shown in Figure 2a. If there is no clear peak, typically a strong impedance contrast (e.g., a soft soil layer over hard rock) is not present at the site. Either the site is a rock site at which no soil site effects are expected or there is gradual increase in shear wave velocity with depth (e.g., gravel transitioning to weathered rock). At many sites, a single strong peak in the mHVSR spectra (refer to Fig. 1 and 2b) is readily identifiable, indicating a single strong impedance contrast (e.g., soil over bedrock). At these locations, the period associated with the peak is assumed to be representative of T_0 at the site.

As shown in Figure 2c, sometimes multiple strong peaks were observed in the mHVSR spectra indicating multiple impedance contrasts at the site. In these cases, the automatic peak search in hvsrpy was constrained to search over narrow frequency bands spanning the troughs on either side of the peak of interest. The lognormal mean frequency, lognormal mean period, and σ_{ln} were evaluated for each peak. For the example (Fig. 2C), the first peak frequency is 0.18 Hz, period is 5.58 s, and σ_{ln} is 0.1 and the second peak frequency is 8.65 Hz, period is 0.12 s, and σ_{ln} is 0.1. Knowledge of the local geologic and geotechnical conditions may provide insight into the observed (or lack of observed) mHVSR peaks and associated frequencies/periods. Identification of T_0 at sites with multiple mHVSR peaks must be linked to the key impedance contrast for site response (often soil over rock).

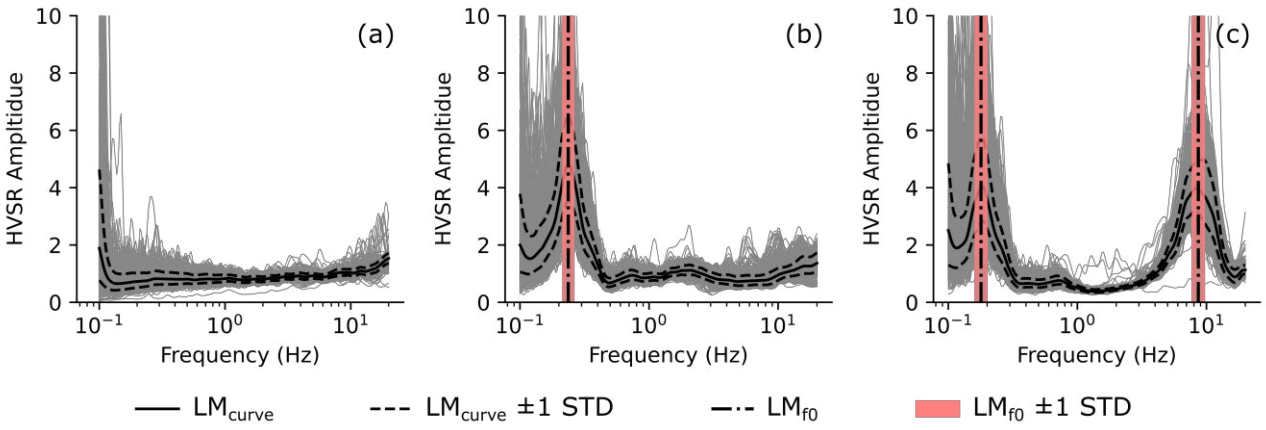

Figure 2: Example mHVSR spectra at sites with (a) zero, (b) one, and (c) two clear peaks.

3 RESULTS & DISCUSSION

3.1 Nationwide Overview

The mHVSR spectra were calculated and examined for clear peaks at each of the 113 sites with suitable ambient vibration data. If one or more peaks were observed in the mHVSR spectra, the lowest frequency (longest period) peak was assumed to be associated with the key impedance contrast for this preliminary overview of the data. As period is more commonly used in engineering practice, Figure 3 is a map of the period associated with the longest period mHVSR peak identified across Aotearoa New Zealand. Darker colours indicate short period values, which are associated with shallow impedance contrasts. At sites with no

clear mHVSR peak, the circular markers are filled with dark grey and noted with NP. Conversely, long period values (i.e., deep impedance contrasts) are indicated by lighter colours.

On the South Island there are three clusters of data: (1) the Southeast portion of the island, including Southland, Otago, and South Canterbury, (2) the centre of the West Coast and Southern Alps, and (3) Marlborough. Periods less than 0.6 s are indicative of shallow soil sites and periods less than 0.1 s or no peak

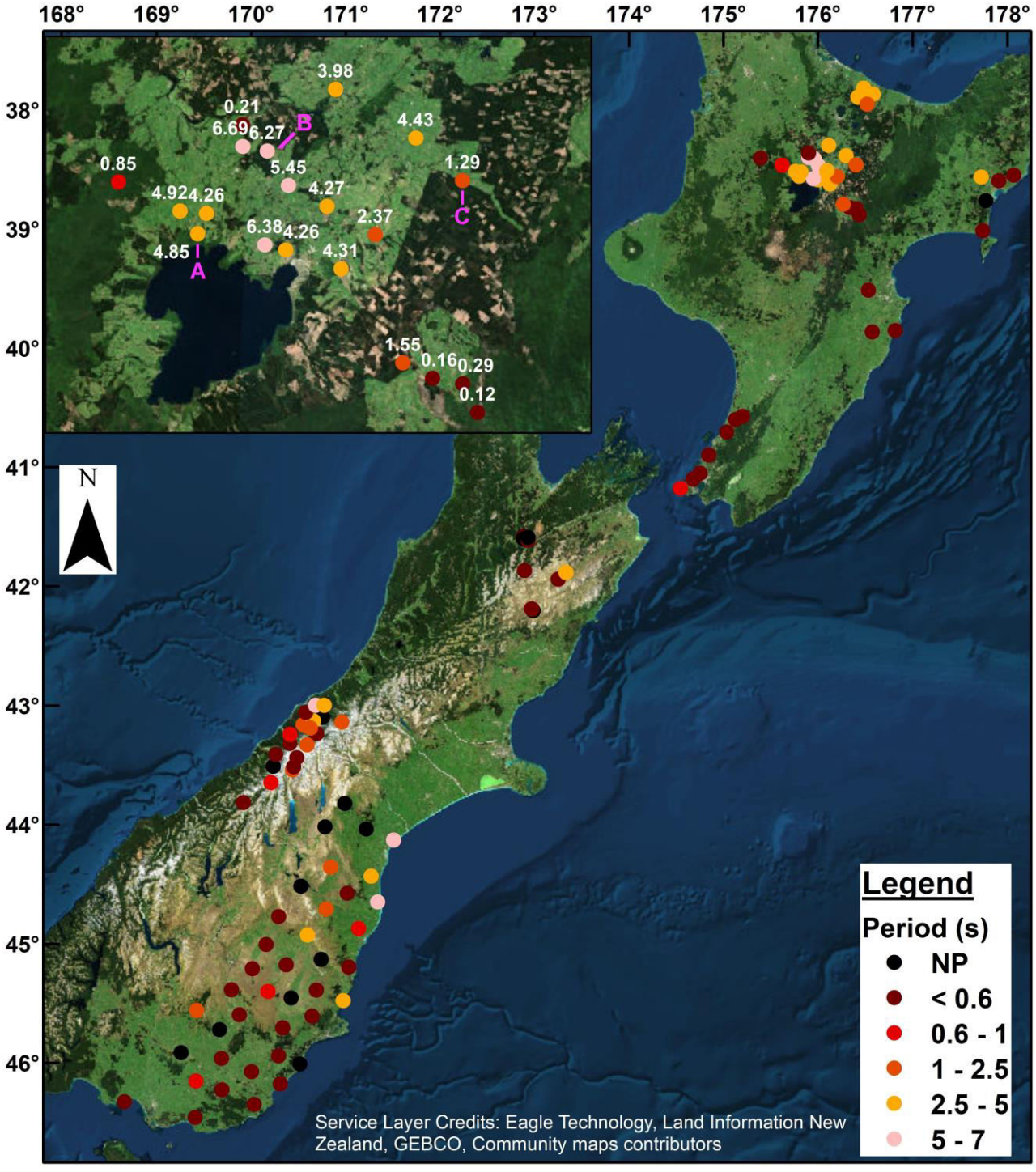

Figure 3: Maps of the New Zealand and (inset) the Taupō Volcanic Zone with circular markers indicating the location of an IRIS temporary station deployment. Marker colour indicates the period associated with the longest period mHVSR peak. The locations of Sites A, B, and C are indicated in the inset.

present are generally indicative of rock sites. In the Southeast of the South Island, many of the sites are in shallow sedimentary basins or on rock outcrops. Notable, exceptions are the coastal deep sedimentary basins. Specifically, the points in the Southern Canterbury Plains (period values of 6.0, 4.2 and, 5.6 s) align with previous observations of the fundamental period of vibration above the greywacke basement bedrock (Stolte et al. 2022). Along the West Coast and in valleys along the Southern Alps the period values are typically low, representative of shallow bedrock. However, there are a few outliers with long period values: 4.6 s near valley near Whataroa, and 6.2 s & 4.0 s in the valley near Harihari. These may be indicative of the deep incised coastal sedimentary basins and further field studies are needed. Lastly, the few locations Marlborough are generally short period, indicating shallow bedrock. The notable exception is a period of 3.5 s at a location in the Awatere Valley, where deeper gravel deposits are present.

The available IRIS data on the North Island is clustered along the Kāpiti Coast, Hawkes Bay, Gisborne, and the Taupō Volcanic Zone. The short period values at sites from Wellington and along the Kāpiti Coast are indicative of the relatively shallow sedimentary basins and much data was collected along the edge of the Tararua Ranges. In Hawkes Bay and Gisborne, again the temporary deployment of sensors focused on testing along basin edges as indicated by the short period values. One notable exception is the period value of 3.3 s in a valley near the town of Ngātapa in the Gisborne District.

3.2 Taupō Volcanic Zone (TPV) and multiple mHVSR peaks

A regional outlier in the period map (Fig. 3) is the TPV (partially shown in the inset of Fig. 3), extending from the northern shores of Lake Taupō to the Bay of Plenty. In the middle of the region, there are long period values, ranging from 4.0 to 6.7 s, which indicates the presence of a deep impedance contrast. Often, there are multiple strong peaks in the mHVSR spectra from sites across the TPV. The mHVSR spectra from three example sites (A, B, and C) are shown in Figure 4, with the associated frequencies and periods summarised in Table 1. The locations of sites A, B and C are indicated in the inset of Figure 3. Sites A and B exhibit clear long period peaks (4.85 and 6.27 s, respectively), indicative of a deep impedance contrast. A shallower “mid” impedance contrast is present at Site B and C. At all three sites, short period peaks indicate the influence of a shallower impedance contrast in the region.

Rosenberg et al. (2020) describe the structural geology of this area, the Wairake-Tauhara geothermal area in the TPV, which is complex due to significant faulting and the interlayering of volcanic rock with fluvial and lacustrine sedimentary deposits. The peaks associated with the longest periods may be attributed to the deep underlying greywacke basement bedrock, which has not been encountered in boreholes up to 3000 m deep. The lateral extent of the lava flows and local sediments varies across the area, but the middle impedance peak periods may be attributed to the impedance contrast between sediments and an underlying dacite or rhyolite volcanic layer. Lastly, the shortest period peaks may be attributed any near-surface soils over the most recent lava flows.

The present study is a preliminary, high-level overview of a nationwide dataset, however, the presence of multiple peaks in the has been observed in other regional studies in Aotearoa New Zealand. Stolte et al. (2022) noted the observation of mHVSR peaks at several locations in the Canterbury Plains and Christchurch. The associated periods were tied to the fundamental period of vibration of soil and weak rock above three key geologic units: the greywacke basement bedrock, the Banks Peninsula Volcanics, and Riccarton Gravel. Following the 2010-2011 Canterbury Earthquake Sequence, the short to mid-range periods of vibration were observed the recordings from many earthquakes including the M_W 6.2 2011 Christchurch EQ, while amplification at the longer periods due to the vibration of the entire column of geologic strata above the basement bedrock was only observed for the largest event, the M_W 7.1 2010 Darfield EQ. When modelling site effects, the metric T_0 should correspond to the key impedance contrast driving the site

response whether this is associated with soil over rock, or soft rock layers over stiffer rock (Wotherspoon et al. 2022).

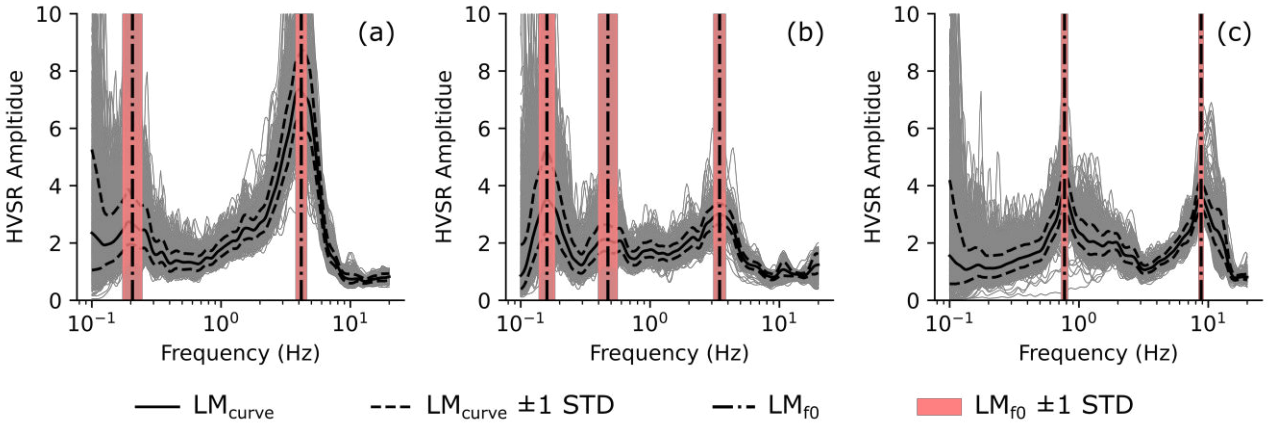

Figure 4: Example mHVSR spectra at three sites (sites A, B, and C) in the TPV with multiple peaks

Table 1: Frequencies & Periods associated with mHVSR peaks at example sites in the TPV

Site ---	f_{deep} (Hz)	T_{deep} (s)	$\sigma_{ln,deep}$ ---	f_{mid} (Hz)	T_{mid} (s)	$\sigma_{ln,mid}$ ---	$f_{shallow}$ (Hz)	$T_{shallow}$ (s)	$\sigma_{ln,shallow}$ ---
A	0.21	4.85	0.16				4.17	0.24	0.08
B	0.16	6.27	0.13	0.47	2.12	0.16	3.45	0.29	0.09
C				0.77	1.29	0.04	8.80	0.03	0.11

4 CONCLUSION

A nationwide dataset of ambient vibration data was collated the publicly available IRIS data service. The data was collected as a part of several studies over the past 30 years for a variety of purposes, using borrowed IRIS broadband instruments. For this preliminary study, day-long ambient vibration records were extracted and processed for 113 locations. The mHVSR method was used to estimate the fundamental period of vibration of soil and rock above one or more key geologic layers. These period estimates provide insight into observed and potential earthquake ground shaking and enable the scoping of future targeted regional dynamic site characterisation studies.

In some locations (e.g., the TPV), multiple peaks in the mHVSR spectra were observed, indicating several key impedance contrasts that may contribute the response of the sedimentary basin and the soil stratigraphy to earthquake ground shaking. This implication of multiple and often deep impedance contrasts is an ongoing area of research, and the present study highlights the need for more experimental and numerical studies.

5 ACKNOWLEDGEMENTS

All seismic data were downloaded through the IRIS Web Services (https://service.iris.edu/), including the following seismic networks: 2B (Illsley-Kemp and Savage, 2019), 2P (Kaneko and Chow, 2017), 6F (Thurber et al., 2012), 6K (Reyners, 2014), 9F (Stern et al., 2008), XF (Jones and Sheehan, 2000), XQ (White 2001), YA (Ebinger and Stern 2017), YR (Bannister 2008), YG (Savage 2013), Z8 (Bannister 2009), ZT (Thurber et al., 2012), and ZX (Townend et al, 2021)

6 REFERENCES

Bannister S (2008). "ALFA08". *International Federation of Digital Seismograph Networks*. https://doi.org/10.7914/SN/YR_2008

Bannister S (2009). "Deep Geothermal HADES seismic array". *International Federation of Digital Seismograph Networks*. https://doi.org/10.7914/SN/Z8_2009

Borcherdt RD (1970). "Effects of local geology on ground motion near San Francisco Bay". *Bulletin of the Seismological Society of America,* **60**(1): 29–61.

Cadet H, Bard PY, Duval AM, and Bertrand E (2012). "Site effect assessment using KiK-net data: part 2—site amplification prediction equation based on f0 and Vsz". *Bulletin of Earthquake Engineering*, **10**(2): 451-489.

Cox BR, Chang T, Vantassel JP, and Manuel L (2020). "A statistical representation and frequency-domain window-rejection algorithm for single-station HVSR measurements". *Geophysical Journal International,* **221**(3): 2170-2183. https://doi.org/10.1093/gji/ggaa119

Ebinger C and Stern T (2017). "Back-arc rifting in New Zealand". *International Federation of Digital Seismograph Networks*. https://doi.org/10.7914/SN/YA_2017

Gregor N, Abrahamson NA, Atkinson GM, Boore DM., Bozorgnia Y, Campbell KW, Chiou BS-J, Idriss IM, Kamai R, Seyhan E, Silva W, Stewart JP, and Youngs R (2014). "Comparison of NGA-West2 GMPEs". *Earthquake Spectra*, **30**(3): 1179-1197. https://doi.org/10.1193/070113EQS186M

Illsley-Kemp F and Savage M (2019). "Eruption or catastrophe: Learning to implement preparedness for future supervolcano eruptions". *International Federation of Digital Seismograph Networks*. https://doi.org/10.7914/SN/2B_2019

Jones C and Sheehan A (2000). "Array studies of anisotropy and converted phases in the Marlborough Fault Zone of New Zealand". *International Federation of Digital Seismograph Networks*. https://doi.org/10.7914/SN/XB_2000

Kaneko Y and Chow B (2017). "Broadband East Coast Network". *International Federation of Digital Seismograph Networks*. https://doi.org/10.7914/SN/2P_2017

Konno K and Ohmachi T (1998). "Ground-motion characteristics estimated from spectral ratio between horizontal and vertical components of microtremor". *Bulletin of the Seismological Society of America*, **88**(1): 228-241.

Kramer SL (1996). *Geotechnical Earthquake Engineering*, Prentice-Hall, Inc. https://doi.org/10.1007/978-3-540-35783-4

Manea EF, Cioflan CO, Coman A, Michel C, Poggi V, and Fäh D (2020). "Estimating geophysical bedrock depth using single station analysis and geophysical data in the extra-Carpathian area of Romania". *Pure and Applied Geophysics*, **177**: 4829-4844.

Manea EF, Cioflan CO, and Danciu, L (2022). "Ground-motion models for Vrancea intermediate-depth earthquakes". *Earthquake Spectra*, **38**(1): 407-431.

Molnar S, Cassidy JF, Castellaro S, Cornou C, Crow H, Hunter JA, Matsushima S, Sánchez-Sesma FJ, and Yong A (2018). "Application of microtremor horizontal-to-vertical spectral ratio (MHVSR) analysis for site characterization: State of the art". *Surveys in Geophysics*, **39**(4): 613-631.

Nakamura Y (1989). "A method for dynamic characteristics estimation of subsurface using microtremor on the ground surface". *Quarterly Report of the Railway Technical Research Institute.* **30**(1): 25-33.

Nakamura Y, (2019). "What is the Nakamura Method?". *Seismological Research Letters*, **90**(4): 1437-1443.

Pitilakis K, Riga E, and Anastasiadis A (2013). "New code site classification, amplification factors and normalized response spectra based on a worldwide ground-motion database". *Bulletin of Earthquake Engineering*, **11**(4), 925-966.

Reyners M (2014). "Otago temporary broadband network". *International Federation of Digital Seismograph Networks*. https://doi.org/10.7914/SN/6K_2014

Rosenberg MD, Wilson CJN, Bignall G, Ireland TR, Sepulveda F, and Charlier BLA (2020). "Structure and evolution of the Wairakei–Tauhara geothermal system (Taupo Volcanic Zone, New Zealand) revisited with a

new zircon geochronology". *Journal of Volcanology and Geothermal Research*, **30**. https://doi.org/10.1016/j.jvolgeores.2019.106705

Savage M (2013). "Deployment for the Southern Cook Strait Earthquake Sequence". *International Federation of Digital Seismograph Networks*. https://doi.org/10.7914/SN/YG_2013

SESAME European project (2004). "*Guidelines for the implementation of the H/V Spectral Ratio Technique on ambient vibrations: measurements, processing and interpretation"*. Deliverable D23.12.

Standards New Zealand (SNZ) (2004). *NZS1170.5 Structural Design Actions. Part 5: Earthquake Actions - New Zealand*. Wellington, NZ.

Stern T, Chamberlain C, Townend J, Michailos K, Boese C. (2008). "Southern Alps microearthquake borehole array - part 2". *International Federation of Digital Seismograph Networks*. https://doi.org/10.7914/SN/9F_2008

Stolte AC, Wotherspoon LM, Cox BR, Wood C, Jeong S, & Munro J (2022). "The influence of multiple impedance contrasts on mHVSR site period estimates in the Canterbury Plains of New Zealand and implications for site classification". *Earthquake Spectra*, https://doi.org/10.1177/87552930221130762

Thurber C, Roecker S, Townend J, Stern T, & Lord N (2012). Wisconsin, New Zealand, and Rensselaer deployment". *International Federation of Digital Seismograph Networks*. https://doi.org/10.7914/SN/ZT_2012

Thurber C, Townend J, and Chamberlain C. (2012). "Wisconsin, New Zealand, and RPI deployment, deep fault drilling project". *International Federation of Digital Seismograph Networks*. https://doi.org/10.7914/SN/6F_2012

Townend J, Holden C, Warren-Smith E, Chamberlain C, Denolle M, & Van Wijk K (2021). "Southern Alps Long Skinny Array; Along-fault array for virtual earthquake analysis of the Alpine Fault". *International Federation of Digital Seismograph Networks*. https://doi.org/10.7914/SN/ZX_2021

Vantassel JP (2020). jpvantassel/hvsrpy: latest (Concept). Zenodo. http://doi.org/10.5281/zenodo.3666956

White, R. (2001). "Hikurangi Subduction System (New Zealand) seismic transects, North Island geophysical transect passive". *International Federation of Digital Seismograph Networks*. https://doi.org/10.7914/SN/XQ_2001

Wotherspoon LM, Kaiser AE, Manea EF, Stolte AC (2022). "*National Seismic Hazard Model: Site Characterisation Database summary report (GNS Science report; 2022/28)"* GNS Science, Lower Hutt, New Zealand, 54 pp. https://doi.org/10.21420/363X-CK83

Zhu C, Pilz M, and Cotton F (2020). "Which is a better proxy, site period or depth to bedrock, in modelling linear site response in addition to the average shear-wave velocity?". *Bulletin of Earthquake Engineering* **18**:797-820. https://doi.org/10.1007/s10518-019-00738-6